



# Hydrogen oxidation kinetics at Ni – Zr<sub>0.9</sub>Sc<sub>0.1</sub>O<sub>1.95</sub> anode: Influence of the difference of potential in the dense part of the double electric layer

D.A. Osinkin <sup>a, b, \*</sup>, B.L. Kuzin <sup>a</sup>

<sup>a</sup> Institute of High-Temperature Electrochemistry, 620137, Yekaterinburg, Russia

<sup>b</sup> Ural Federal University, 620002, Yekaterinburg, Russia

## ARTICLE INFO

### Article history:

Received 5 March 2018

Received in revised form

5 June 2018

Accepted 6 June 2018

Available online 7 June 2018

### Keywords:

Ni – SSZ anode

Point of zero charge

Rate-limiting step

Double electric layer

DRT

## ABSTRACT

The electrochemical behavior of Ni – Zr<sub>0.9</sub>Sc<sub>0.1</sub>O<sub>1.95</sub> anode in contact with the YSZ electrolyte was studied in H<sub>2</sub> + H<sub>2</sub>O + Ar mixtures at 900 °C by means of impedance spectroscopy. The analysis of the impedance spectra performed by the distribution of relaxation times and non-linear least square methods demonstrated that the electrode process is limited by several rate-determining steps. High-frequency resistance at equilibrium potential does not depend on the gas mixture composition, whereas low-frequency resistance has the 0.5 reaction order and depends on the water partial pressure. The distribution of relaxation times dependencies under polarization demonstrated that the frequency range of the high-frequency step does not depend on the electrode potential and the contribution of the low-frequency step decreases as the cathode polarization increases. An anomalous behavior of the hydrogen oxidation and water reduction rates in the point of zero charge was observed. The abnormal behavior of polarization curves is for the first time explained by the influence of the difference of potential in the dense part of the double electric layer.

© 2018 Elsevier Ltd. All rights reserved.

## 1. Introduction

In recent years, Ni – based composites (Ni – cermets) have been the basic material for anodes of solid oxide fuel cells (SOFC) - devices, which transform chemical energy into electricity. Ni – cermets are actual due to their high activity toward hydrogen oxidation, they display high electrical conductivity and phase stability in fuel gases [1,2]. Ni – cermets have been widely studied [3–10], but there is a lack of published data on the study of the limiting steps and mechanisms of electrode reactions. In the case of Ni – cermet being in contact with an oxygen-conducting electrolyte, there are conflicting opinions relative to the nature of the hydrogen oxidation limiting steps. Bessler et al. [11] proposed that the Ni surface reactions involving adsorbed water limited the rate of the anode reaction. Mogensen [12] proposed that the increase in the anode reaction rate may be due to the uptake of water into impurity phases. Goodwin et al. [13] assumed that the process of hydroxyl transition to the YSZ surface, which is a subsequent transition back to the Ni surface with water formation on the Ni

surface, may limit the anode reaction. Mizusaki et al. [14,15] and Bieberle [16] consider that the hydrogen adsorption and diffusion on the Ni surface are the rate-determining stages, whereas Jiang et al. [17] report that processes at the electrolyte surface are the rate-determining ones. Boer [18] and Holtappels et al. [19] supposed that the formation of interstitial hydrogen and hydroxyl in the electrolyte are the rate-determining stages. The hydrogen-spillover mechanism first proposed by Mogensen et al. [20], i.e. the mechanism of hydrogen oxidation, which includes the stage of adsorbed hydrogen transition as the proton migration along the Ni surface, should also be mentioned. Vogler et al. [21] assumed that the hydrogen spillover with water formation at the YSZ surface may explain the relationship between the polarization resistance and H<sub>2</sub> and H<sub>2</sub>O partial pressures. Shishkin et al. [22] proposed that the H<sub>2</sub> oxidation at the Ni/ZrO<sub>2</sub> interface may limit the anode reaction. Based on the density functional theory study [22] the oxygen vacancy formation at the interface of Ni/YSZ was shown to be more favorable than that at the YSZ surface. Also it was found that the energy barrier for water formation at the Ni/YSZ boundary is lower than that at Ni or YSZ surface. This implies that the step of charge transfer occurring at the interface is more feasible than oxygen and hydrogen spillover pathways.

We have previously studied in detail the gas-diffusion stage of

\* Corresponding author. Institute of High-Temperature Electrochemistry, 620137, Yekaterinburg, Russia.

E-mail address: [OsinkinDA@mail.ru](mailto:OsinkinDA@mail.ru) (D.A. Osinkin).

the electrode reaction at the impregnated with  $\text{CeO}_2$  Ni – cermet anode in contact with YSZ [23] and made some assumptions relative to the nature of the limiting steps at the Ni – YSZ anodes with cerium oxide addition in  $\text{H}_2 + \text{H}_2\text{O} + \text{CO} + \text{CO}_2$  at the equilibrium potential [24]. In the present work the nature of the rate-determining stages of hydrogen oxidation (water reduction) at the Ni –  $\text{Zr}_{0.9}\text{Sc}_{0.1}\text{O}_{1.95}$  anode in contact with the YSZ electrolyte both at the equilibrium potential and during polarization will be discussed.

## 2. Experimental

### 2.1. Samples preparation

Commercial NiO and  $\text{Zr}_{0.9}\text{Sc}_{0.1}\text{O}_{1.95}$  (SSZ) powders with specific surface areas of 6.9 and  $2.3 \text{ m}^2 \text{ g}^{-1}$ , respectively, were used for the anode preparation. The composite 56% NiO +44% SSZ (wt. %) powder was obtained by mixing of NiO and SSZ in a planetary ball mill (PM 100, Retsch). An electrode slurry was prepared by mixing the electrode powder with isopropyl alcohol and polyvinyl butyral. The slurry was painted onto both sides of a dense (about 95% of the crystallographic density) plate of a commercial YSZ electrolyte. After drying, the electrodes were sintered at  $1250 \text{ }^\circ\text{C}$  for 2 h in air. The resulting electrode thickness was about  $30 \text{ }\mu\text{m}$  with the dimensions of about  $0.5 \times 0.5 \text{ cm}^2$ . After that, platinum wire (diameter 0.01 cm) was fixed by platinum paste to the YSZ perimeter and served as a reference electrode. The reference electrode was fired at  $1000 \text{ }^\circ\text{C}$  for 1 h in air. The electrode reduction was performed in wet ( $p_{\text{H}_2\text{O}} = 0.03 \text{ atm}$ ) hydrogen for 1 h at  $900 \text{ }^\circ\text{C}$ . The anode composition after reduction was 50% Ni + 50% SSZ (Ni – SSZ).

### 2.2. Measurements

Investigations were performed in  $\text{H}_2 + \text{H}_2\text{O} + \text{Ar}$  mixtures. For the gas mixture preparation Ar and  $\text{H}_2$  (purity not less than 99.99 vol%) were used. The hydrogen and argon partial pressures were set by the highly accurate flow-measuring devices produced by the Bronkhorst company. The amount of water in the gas mixture was regulated by controlling the temperature of the saturator, through which the  $\text{H}_2 + \text{Ar}$  flow was passing. The oxygen activity in the gas mixture was measured by a solid oxide oxygen sensor, which was placed near the studied samples. The internal volume of the sensor was purged with air. All measurements were carried out at atmospheric pressure. A measurement setup was similar to that described in Ref. [25] and shown in Fig. 1. Unlike

$\text{H}_2 + \text{H}_2\text{O}$  gas mixtures, in which the partial pressure of the components can be easily calculated using the equations given in Ref. [26], in  $\text{H}_2 + \text{H}_2\text{O} + \text{Ar}$  mixtures, a different approach is needed to determine the partial pressures of hydrogen and water. The approach to calculate the partial pressures of hydrogen and water is provided in the Appendix.

The electrochemical characteristics were studied by means of impedance spectroscopy in the frequency range of  $10^5$ – $10^{-1} \text{ Hz}$  using FRA-1260 and EI-1287 (Solartron). The cell was connected to the electrochemical interface in the two-electrode four-wire mode, which permitted to exclude the impedance of current-supplying cables from the overall impedance. Pt mesh and wires were used as current collectors and leads. The anode and cathode polarization dependencies were investigated on different symmetrical cells. Polarization dependencies were measured only for one Ni – SSZ electrode of a symmetrical cell, the second Ni – SSZ electrode served as a counter electrode. The current and voltage values during polarization measurements were recorded at a zero value of the impedance imaginary component at high frequencies. When the spectrum was measured the polarization was turned off. The next measurement was performed at the electrodes in the equilibrium state. The overvoltage  $\eta$  was calculated according to equation (1):

$$\eta = U - IR_s \quad (1)$$

where  $U$  is the difference of potentials between the Ni–SSZ and reference electrodes,  $I$  is the current,  $R_s$  is the series resistance detected according to the place where high-frequency impedance spectrum crossed the axis of abscissa.

For the distribution of relaxation time (DRT) analysis a program code, developed by the authors of [27], based on the Tikhonov's regularization [28] was applied. The Z-View software was used to analyze the impedance spectra by the non-linear least square method.

A SEM images of the cell cross-section was obtained on a Jeol JSM 5900LV scanning electron microscope.

## 3. Results

### 3.1. Result of measurements under equilibrium potential

A typical impedance spectrum of the Ni – SSZ electrode is shown in Fig. 2. It is seen that the spectrum does not have pronounced semicircles, which makes it difficult to choose the equivalent circuit for its analysis by the non-linear least square (NLLS) method. The method of distribution relaxation times (DRT),

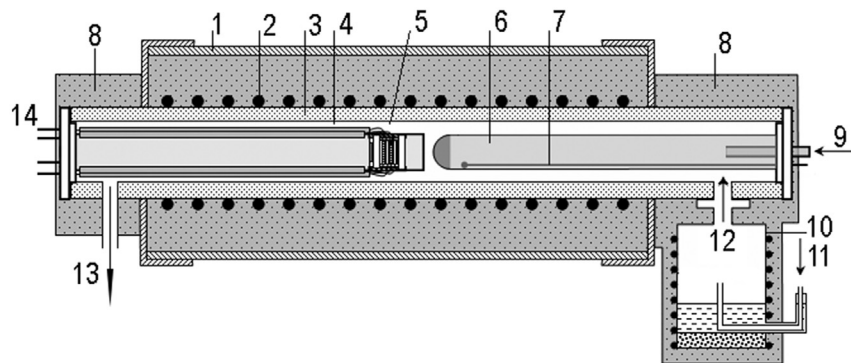


**Fig. 1.** Sketch of measuring setup: 1 - furnace, 2 - heating element, 3 - alumina tube, 4 - measuring rig, 5 - samples, 6 - sensor of partial oxygen pressure, 7 - thermocouple, 8 - thermal insulation, 9 - air supply to the sensor, 10 - saturator with heating element, 11 -  $\text{H}_2 + \text{Ar}$  feeding, 12 -  $\text{H}_2 + \text{H}_2\text{O} + \text{Ar}$  feeding, 13 -  $\text{H}_2 + \text{H}_2\text{O} + \text{Ar}$  outlet, 14 - leads to FRA-1260 and EI-1287 (Solartron).

Download English Version:

<https://daneshyari.com/en/article/6602135>

Download Persian Version:

<https://daneshyari.com/article/6602135>

[Daneshyari.com](https://daneshyari.com)